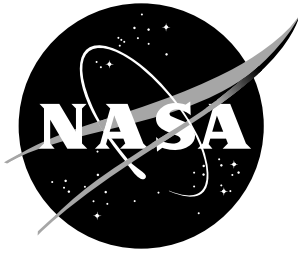# Application of AWE Along with a Combined FEM/MoM Technique to Compute RCS of a Cavity-Backed Aperture in an Infinite Ground Plane Over a Frequency Range

C. J. Reddy
Hampton University, Hampton, Virginia

M. D. Deshpande
ViGYAN, Inc., Hampton, Virginia

December 1997

The NASA STI Program Office ... in Profile

Since its founding, NASA has been dedicated to the advancement of aeronautics and space science. The NASA Scientific and Technical Information (STI) Program Office plays a key part in helping NASA maintain this important role.

The NASA STI Program Office is operated by Langley Research Center, the lead center for NASA's scientific and technical information. The NASA STI Program Office provides access to the NASA STI Database, the largest collection of aeronautical and space science STI in the world. The Program Office is also NASA's institutional mechanism for disseminating the results of its research and development activities. These results are published by NASA in the NASA STI Report Series, which includes the following report types:
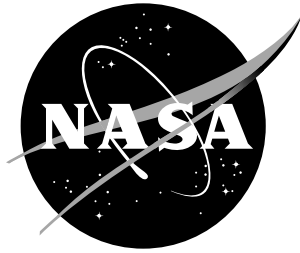
- TECHNICAL PUBLICATION. Reports of completed research or a major significant phase of research that present the results of NASA programs and include extensive data or theoretical analysis. Includes compilations of significant scientific and technical data and information deemed to be of continuing reference value. NASA counter-part of peer reviewed formal professional papers, but having less stringent limitations on manuscript length and extent of graphic presentations.

- TECHNICAL MEMORANDUM. Scientific and technical findings that are preliminary or of specialized interest, e.g., quick release reports, working papers, and bibliographies that contain minimal annotation. Does not contain extensive analysis.

- CONTRACTOR REPORT. Scientific and technical findings by NASA-sponsored contractors and grantees.

- CONFERENCE PUBLICATION. Collected papers from scientific and technical conferences, symposia, seminars, or other meetings sponsored or co-sponsored by NASA.

- SPECIAL PUBLICATION. Scientific, technical, or historical information from NASA programs, projects, and missions, often concerned with subjects having substantial public interest.

- TECHNICAL TRANSLATION. English-language translations of foreign scientific and technical material pertinent to NASA's mission.

Specialized services that help round out the STI Program Office's diverse offerings include creating custom thesauri, building customized databases, organizing and publishing research results ... even providing videos.

For more information about the NASA STI Program Office, you can:

- Access the NASA STI Program Home Page at http://www.sti.nasa.gov/STI-homepage.html

- E-mail your question via the Internet to help@sti.nasa.gov

- Fax your question to the NASA Access Help Desk at (301) 621-0134

- Phone the NASA Access Help Desk at (301) 621-0390

- Write to:
  NASA Access Help Desk
  NASA Center for AeroSpace Information
  800 Elkridge Landing Road
  Linthicum Heights, MD 21090-2934

Application of AWE Along with a Combined FEM/MoM Technique to Compute RCS of a Cavity-Backed Aperture in an Infinite Ground Plane Over a Frequency Range

C. J. Reddy
Hampton University, Hampton, Virginia

M. D. Deshpande
ViGYAN, Inc., Hampton, Virginia

December 1997

CONTENTS

Abstract

A hybrid Finite Element Method (FEM)/Method of Moments (MoM) technique in conjunction with the Asymptotic Waveform Evaluation (AWE) technique is applied to obtain radar cross section (RCS) of a cavity-backed aperture in an infinite ground plane over a frequency range. The hybrid FEM/MoM technique when applied to the cavity-backed aperture results in an integro-differential equation with electric field as the unknown variable, the electric field obtained from the solution of the integro-differential equation is expanded in Taylor series. The coefficients of the Taylor series are obtained using the frequency derivatives of the integro-differential equation formed by the hybrid FEM/MoM technique. The series is then matched via the Padé approximation to a rational polynomial, which can be used to extrapolate the electric field over a frequency range. The RCS of the cavity-backed aperture is calculated using the electric field at different frequencies. Numerical results for a rectangular cavity, a circular cavity, and a material filled cavity are presented over a frequency range. Good agreement between AWE and the exact solution over the frequency range is obtained.

List of Symbols

∇	Del operator
∇'	Del operator over the source coordinates
ε_r	Dielectric permittivity of the medium in the cavity
δ_{qo}	Kronecker delta defined in equation (23)
μ_o	Magnetic permeability of free space
μ_r	Dielectric permeability of the medium in the cavity
η_o	Intrinsic impedance of free space
θ_i	Incident angle in θ direction
ϕ_i	Incident angle in ϕ direction
$\hat{\theta}$	Unit normal along θ direction
$\hat{\phi}$	Unit normal along ϕ direction
ω	Angular frequency
AWE	Asymptotic Waveform Evaluation
$A^{(q)}(k_o)$	qth derivative of $A(k)$ with respect to k; $\dfrac{d^q}{dk^q}A(k)$, evaluated at k_o
$b(k)$	Excitation vector
$b^{(q)}(k_o)$	qth derivative of $b(k)$ with respect to k; $\dfrac{d^q}{dk^q}b(k)$, evaluated at k_o
ds	Surface integration with respect to observation coordinates
ds'	Surface integration with respect to source coordinates
$\mathbf{E}$	Electric field
E_{inc}	Incident electric field
$e(k)$	Electric field coefficient vector
$\mathbf{H}_{inc}$	Incident magnetic field at the surface S_{inc}

$\mathbf{H}_{scat}$	Scattered magnetic field
H_{xi}	x-component of the incident magnetic field
H_{yi}	y-component of the incident magnetic field
H_{zi}	z-component of the incident magnetic field
$H_{\theta i}$	θ-component of the incident magnetic field
$H_{\phi i}$	φ-component of the incident magnetic field
$H_{\theta s}$	Scattered magnetic field in θ direction
$H_{\phi s}$	Scattered magnetic field in φ direction
FDTD	Finite Difference Time Domain
FEM	Finite Element Method
f	Frequency
j	$\sqrt{-1}$
$\mathbf{k}_i$	As defined in equation (11)
k	Wavenumber at any frequency f
k_o	Wavenumber at frequency f_o
MoM	Method of Moments
$\mathbf{M}$	Magnetic current at the surface S_{ap}
m_n	n^{th} moment of AWE ($n=0,1,2,3,4$ ....)
$\hat{\mathbf{n}}$	Normal unit vector
PEC	Perfect Electric Conductor
$P_L(.)$	Polynomial of order L
$Q_M(.)$	Polynomial of order M
$q!$	Factorial of number q

RCS	Radar Cross Section
R	Distance between the source point and the observation point
$\mathbf{T}$	Vector testing function
$\mathbf{T}_s$	Vector testing function at the surface S_{ap}
VLSI	Very Large Scale Integrated (circuits)
$\mathbf{z}$	Unit normal along Z-axis

1. Introduction

The electromagnetic characterization of cavity backed apertures is of importance in understanding the scattering properties and in electromagnetic penetration/coupling studies. Recently, there has been a considerable interest in analyzing cavity backed apertures in an infinite ground plane. Various analytical and numerical techniques have been applied for two dimensional cavity backed apertures [1-6]. For three dimensional problems, mode matching has been used for rectangular [7] and spherical [8] cavity backed apertures. A Method of Moments (MoM)/modal [9] approach is used recently to analyze apertures formed by a rectangular cavity recessed in a ground plane. These methods are restricted to cavities with regular shapes, where fields can be written in modal form. In [10], a boundary integral method is used to analyze the scattering from three dimensional cavities via a connection scheme. Though useful for savings in computer memory, this method leads to dense matrices. Also, the accumulation errors due to the connection algorithm are not negligible as the number of subsections increase. In the case of deep cavities, high frequency techniques such as those proposed in [11] and [12] could be effectively implemented. Unfortunately, these techniques are not suitable when the cavity is filled with inhomogeneous materials. In [13], a Finite Difference Time Domain (FDTD) method is applied for large structures. However, the method of FDTD sometimes results in inaccurate results due to differencing, staircasing and dispersion. Jin and Volakis [14] used a finite element-boundary integral formulation which employs the boundary integral equation (or Method of Moments-MoM) to formulate the fields external to the cavity accurately.

In the combined FEM/MoM technique, FEM is used in the cavity volume to compute the electric field, whereas MoM is used to compute the magnetic current at the aperture. For the combined FEM/MoM technique, the cavity is divided into tetrahedral elements and the aperture

is discretized by triangles. Using the Galerkin's technique, simultaneous equations are generated over the subdomains and are added to form a global matrix equation. This results in a partly sparse and partly dense, symmetric complex matrix, which can be solved either by a direct solver or by an iterative solver. The electric field hence obtained is used to compute the RCS of the cavity-backed aperture.

To obtain RCS over a range of frequencies using the combined FEM/MoM technique, one has to repeat the calculations over the frequency range of interest. If the RCS is highly frequency dependent, one needs to do the calculations at the finer increments of frequency to get the accurate representation of the frequency response. This can be computationally intensive and for an electrically large cavity with electrically large aperture, it can be computationally prohibitive despite the increased power of the present generation of computers. To alleviate the above problems, the application of Asymptotic Waveform Evaluation (AWE) has been proposed for the timing analysis of VLSI circuits [15]. The AWE technique is finding increasing interest in electromagnetic analysis of microwave circuits [16-18]. Recently a detailed description of AWE applied to frequency domain electromagnetic analysis is presented in [19]. AWE has been used to predict RCS of PEC bodies over a frequency range [20] and input characteristics of a cavity-backed aperture antenna over a frequency range [21].

In this report, the application of AWE for predicting the RCS over a range of frequencies for a cavity-backed aperture using a combined FEM/MoM technique is described. In the AWE technique, the electric field is expanded in a Taylor series around a frequency. The coefficients of the Taylor series (called 'moments') are evaluated using the frequency derivatives of the combined FEM/MoM equation. These moments are then matched via the Padé approximation to a rational polynomial. Using the rational polynomial, the electric field distribution in the cavity

7

can be obtained over a frequency range. Using this field distribution, the RCS of the cavity-backed aperture in an infinte ground plane is calculated at any frequency within the frequency range.

The rest of the report is organized as described below. A brief description of hybrid FEM/MoM technique to calculate RCS from a cavity-backed aperture is given in section 2. In section 3, AWE implementation for the combined FEM/MoM technique is described. Numerical results for a rectangular cavity, a circular cavity, and a material filled cavity are presented in section 4. The numerical data are compared with the exact solution (calculated at each frequency using the hybrid FEM/MoM technique) over the frequency range. CPU time and storage requirements for AWE formulation are given for each example and are compared with those required for exact solution at each frequency. Concluding remarks on the AWE technique are presented in section 5.

2. Hybrid FEM/MoM Technique

The geometry of the problem to be analyzed is shown in figure 1. For linear, isotropic, and source free region, the electric field satisfies the vector wave equation:

$$\nabla \times \left(\frac{1}{\mu_r} \nabla \times \mathbf{E} \right) - k^2 \varepsilon_r \mathbf{E} = 0 \tag{1}$$

where μ_r, ε_r are the relative permeability and relative permittivity of the medium in the cavity and k is the free space wavenumber. The time variation $\exp(j\omega t)$ is assumed and suppressed throughout this paper. The electric field $\mathbf{E}$ is solved via hybrid FEM/MoM technique assuming that cavity-backed aperture is illuminated by a harmonic plane wave, $\mathbf{H}_{inc}$. Following the procedure described in [14], equation (1) can be written as

$$\iiint_V (\nabla \times \mathbf{T}) \bullet \left(\frac{1}{\mu_r} \nabla \times \mathbf{E} \right) dv - k_o^2 \varepsilon_r \iiint_V \mathbf{T} \bullet \mathbf{E} dv - j\omega\mu_o \iint_{S_{ap}} (\mathbf{T} \times \hat{\mathbf{n}}) \bullet \mathbf{H}_{scat} ds$$

$$= 2j\omega\mu_o \iint_{S_{ap}} (\mathbf{T} \times \hat{\mathbf{n}}) \bullet \mathbf{H}_{inc} ds \tag{2}$$

where $\mathbf{T}$ is the vector testing function. S_{ap} is the aperture surface (see figure 1). $\mathbf{H}_{scat}$ is the scattered magnetic field and $\hat{\mathbf{n}} = \hat{\mathbf{z}}$ at S_{ap}.

The volume of the cavity is subdivided into small volume tetrahedral elements. The electric field is expressed in terms of the edge vector basis functions [22], which enforce the divergenceless condition of the electric field explicitly. The vector testing function is also expressed in terms of the edge vector basis functions following the Galerkin's method. The discretization of the cavity volume into tetrahedral elements automatically results in discretization of the surface S_{ap} into triangular elements. The volume and surface integrals in equation (2) are carried out over each element to form element matrices, which are assembled to form global matrices. Equation (2) can be written in matrix form as

$$A(k)\,e(k) \;=\; b(k) \tag{3}$$

$A(k)$ is a partly sparse, partly dense complex symmetric matrix, $b(k)$ is the excitation vector, and $e(k)$ is the unknown electric field coefficient vector. $A(k)$ is evaluated as a sum of three matrices.

$$A(k) \;=\; A_1(k) + A_2(k) + A_3(k) \tag{4}$$

where

$$A_1(k) \;=\; \iiint_V (\nabla \times \mathbf{T}) \bullet \left(\frac{1}{\mu_r}\nabla \times \mathbf{E}\right)dv - k^2\varepsilon_r\iiint_V \mathbf{T} \bullet \mathbf{E}\,dv \tag{5}$$

$$A_2(k) \;=\; -\frac{k^2}{2\pi}\iint_{S_{ap}} \mathbf{T}_s \bullet \left(\iint_{S_{ap}} \mathbf{M}\frac{\exp(-jkR)}{R}ds'\right)ds \tag{6}$$

$$A_3(k) \;=\; \frac{1}{2\pi}\iint_{S_{ap}} (\nabla\bullet\mathbf{T}_s)\left\{\iint_{S_{ap}} (\nabla' \bullet \mathbf{M})\frac{\exp(-jkR)}{R}ds'\right\}ds \tag{7}$$

$$b(k) \;=\; 2j\omega\mu_o\iint_{S_{ap}} (\mathbf{T} \times \hat{\mathbf{n}}) \bullet \mathbf{H}_{inc}\,ds \tag{8}$$

Equations (6) and (7) are obtained by making use of the equivalence principle and image theory [23] and follow the procedure given in [24]. $\mathbf{T}_s = \mathbf{T} \times \hat{\mathbf{n}}$ and R is the distance between source point and the observation point. $\mathbf{M}$ is the equivalent magnetic current over the aperture S_{ap}. ∇' indicates del operation over the source coordinates and ds' indicates the surface integration over the source region. Equation (8) is calculated assuming a harmonic plane wave

$$\mathbf{H}_{inc} \;=\; (\hat{\mathbf{x}}H_{xi} + \hat{\mathbf{y}}H_{yi} + \hat{\mathbf{z}}H_{zi})\,e^{-j\mathbf{k}_i \bullet \mathbf{r}} = \left(\hat{\theta}H_{\theta i} + \hat{\phi}H_{\phi i}\right)e^{-j\mathbf{k}_i \bullet \mathbf{r}} \tag{9}$$

$$\mathbf{E}_{inc} \;=\; \eta_o\mathbf{H}_{inc} \times \mathbf{k}_i \tag{10}$$

where

$$\mathbf{k}_i = -k_o\left[\hat{\mathbf{x}}\sin\theta_i\cos\phi_i + \hat{\mathbf{y}}\sin\theta_i\sin\phi_i + \hat{\mathbf{z}}\cos\theta_i\right] \tag{11}$$

$$H_{xi} = \left(\sin\alpha\cos\theta_i\cos\phi_i + \cos\alpha\sin\phi_i\right)/\eta_o \tag{12}$$

$$H_{yi} = \left(\sin\alpha\cos\theta_i\sin\phi_i - \cos\alpha\cos\phi_i\right)/\eta_o \tag{13}$$

$$H_{zi} = \left(-\sin\alpha\sin\theta_i\right)/\eta_o \tag{14}$$

$$H_{\theta i} = \left|\mathbf{H}_{inc}\right|\sin\alpha \tag{15}$$

$$H_{\phi i} = \left|\mathbf{H}_{inc}\right|\cos\alpha \tag{16}$$

in which η_o is the free space intrinsic impedance and α represents the polarization angle of the incident field. When $\alpha = 0$, then $H_{zi} = 0$ which corresponds to H-polarization and when $\alpha = \pi/2$, then $E_{zi} = 0$ which corresponds to E-polarization.

The matrix equation (3) is solved at any specific frequency, f_o (with wavenumber k_o) either by a direct method or by an iterative method. The solution of the equation (3) gives the unknown electric field coefficients which are used to obtain the electric field distribution. Once the electric field $\mathbf{E}$ is found and hence the magnetic current $\mathbf{M}$ on the aperture, the far zone scattered field can be computed.

$$\mathbf{H}_{scat}(\mathbf{r})\big|_{r\to\infty} = -\frac{jk_o}{\eta_o}\frac{e^{-jk_or}}{2\pi r}\iint\limits_{S_a}(\hat{\theta}\hat{\theta} + \hat{\phi}\hat{\phi})\bullet\mathbf{M}(x,y)\,e^{jk_o\sin\theta\,(x\cos\phi + y\sin\phi)}\,dxdy \tag{17}$$

where (r, θ, ϕ) are the usual spherical coordinates of the observation point. The scattering cross section is then given by

$$\sigma = \lim_{r\to\infty} 4\pi r^2\frac{\left|\mathbf{H}_{scat}(\mathbf{r})\right|^2}{\left|\mathbf{H}_{inc}(\mathbf{r})\right|^2} \tag{18}$$

11

where

$$|\mathbf{H}_{scat}(\mathbf{r})|^2 = |H_{\theta s}|^2 + |H_{\phi s}|^2 \qquad (19)$$

$$|\mathbf{H}_{inc}(\mathbf{r})|^2 = |H_{\theta i}|^2 + |H_{\phi i}|^2 \qquad (20)$$

3. AWE Implementation

The RCS given in equation (18) is calculated at one frequency. If one needs RCS over a frequency range, this calculation is to be repeated at different frequency values. Instead, AWE can be applied to obtain the frequency response over a frequency range. The general implementation of AWE for any frequency domain technique used for electromagnetic analysis is given in detail in [19]. The solution of equation (3) gives the unknown electric field coefficient vector $e(k_o)$ at a particular frequency f_o. Instead $e(k)$ can be expanded in Taylor series as

$$e(k) = \sum_{n=0}^{\infty} m_n (k - k_o)^n \qquad (21)$$

with the moments m_n given by [19]

$$m_n = A^{-1}(k_o) \left[\frac{b^{(n)}(k_o)}{n!} - \sum_{q=0}^{n} \frac{(1 - \delta_{qo}) A^{(q)}(k_o) m_{n-q}}{q!} \right] \qquad (22)$$

$A^{(q)}(k_o)$ is the qth derivative with respect to k of $A(k)$ given in equation (4) and evaluated at k_o. Similarly, $b^{(q)}(k_o)$ is the qth derivative with respect to k of $b(k)$ given in equation (9) and evaluated at k_o. The Kronecker delta δ_{qo} is defined as

$$\delta_{qo} = \begin{cases} 1 & q = 0 \\ 0 & q \neq 0 \end{cases} \qquad (23)$$

The qth derivatives of $A(k)$ and $b(k)$ are evaluated and are given in detail in the Appendix.

12

In many cases, the Taylor series expansion gives fairly good results. However, the accuracy of the Taylor series is limited by the radius of convergence. It will not converge to the right answer beyond the radius of convergence, and it sometimes requires a large number of terms to converge over a frequency range. In such cases, one may want to replace Taylor series expansion with a rational function called Padé approximation [15] to improve the accuracy of the numerical solution.

To obtain Padé approximation, the Taylor series expansion in equation (21) is matched with a rational polynomial [15]

$$\sum_{n=0}^{\infty} m_n (k-k_o)^n = \frac{P_L (k-k_o)}{Q_M (k-k_o)} \tag{24}$$

where

$$P_L (k-k_o) = a_o + a_1 (k-k_o) + a_2 (k-k_o)^2 + \ldots\ldots + a_L (k-k_o)^L$$

and

$$Q_M (k-k_o) = b_o + b_1 (k-k_o) + b_2 (k-k_o)^2 + \ldots\ldots + b_M (k-k_o)^M$$

b_o is set to 1 as the rational function can be divided by an arbitrary constant. Since there are $(L+M+1)$ unknowns, $(L+M)$ moments of the Taylor series should be matched. Equating the coefficients for powers $(k-k_o)^{L+1}\ldots\ldots (k-k_o)^{L+M}$, the coefficients of $Q_M (k-k_o)$ can be obtained solving the matrix equation

$$\begin{bmatrix} m_{L-M+1} & m_{L-M+2} & \cdots & m_L \\ m_{L-M+2} & m_{L-M+3} & \cdots & m_{L+1} \\ \cdots & \cdots & \cdots & \cdots \\ m_L & m_{L+1} & \cdots & m_{L+M-1} \end{bmatrix} \begin{bmatrix} b_M \\ b_{M-1} \\ \cdots \\ b_1 \end{bmatrix} = - \begin{bmatrix} m_{L+1} \\ m_{L+2} \\ \cdots \\ m_{L+M} \end{bmatrix} \tag{25}$$

The numerator coefficients can be found by equating the powers $(k - k_o)^0 \ldots\ldots\ldots (k - k_o)^L$

$$a_o = m_o$$

$$a_1 = m_1 + b_1 m_o$$

$$a_2 = m_2 + b_1 m_1 + b_2 m_o$$

$$a_L = m_L + \sum_{i = 1}^{min\,(L, M)} b_i m_{L - i}$$

Once the coefficients of the rational polynomial are obtained, equation (21) can be rewritten as

$$e(k) = \frac{a_o + a_1(k - k_o) + a_2(k - k_o)^2 + \ldots\ldots + a_L(k - k_o)^L}{1 + b_1(k - k_o) + b_2(k - k_o)^2 + \ldots\ldots + b_M(k - k_o)^M} \tag{26}$$

For a given amount of computational effort, one can easily construct a rational approximation which has smaller error than a polynomial approximation. Also for a fixed value of *L+M*, the error is smallest when *L=M* or *L=M+1*[17]. Using equation (26), the electric field coefficients at frequencies around the expansion frequency are obtained. The electric field hence obtained is used to compute the scattered magnetic field given in equation (17) and finally the backscattering cross section using equation (18).

4. Numerical Results

To validate the analysis presented in the previous sections, a few examples are considered. RCS calculations over a frequency range are done for a rectangular cavity, a circular cavity, and a cavity filled with lossy material. The numerical data obtained using AWE are compared with the results calculated at each frequency using the computer code CBS3DS [25], which implements the combined FEM/MoM technique [14]. We will refer to the latter method as "exact solution."

From section 3, it can be observed that the inverse of matrix $A(k_o)$ is found once and is used repeatedly to find AWE moments. Due to the hybrid FEM/MoM technique, matrix $A(k_o)$ is partly sparse and partly dense. The Complex Vector Sparse Solver (CVSS) [26] is used to LU factor the matrix $A(k_o)$ once and the moments are obtained by backsolving equation (21) with multiple righthand sides. All the computations reported below are done on a SGI-*Indigo2* (with 150MHz, IP22 processor) computer.

(a) Square Cavity: A square cavity in an infinite ground plane is considered (fig. 2 with *a=1cm, b=1cm,* and *c=2cm*). Backscattering calculations are done with an incident angle $\theta = 0^o$ and $\phi = 0^o$. The discretization of the square cavity resulted in 3590 total unknowns, and the order of the dense matrix due to MoM is 133. Figure 3a shows the radar cross section over the frequency range 15GHz to 25GHz, calculated using Taylor series for a H-polarized incident wave. The Taylor series moments are calculated at 20GHz. Figure 3b shows the radar cross section over the frequency range 15GHz to 25GHz calculated using Padé approximation. It can be seen from Figure 2b that Taylor series gave good results over the frequency range 18GHz to 22GHz. Beyond this frequency range, there is no improvement in accuracy, even by adding more terms to the Taylor series. However, figure 3b indicates that Padé approximation gave good results over the frequency range 15GHz to 25GHz with *L=5* and *M=5*, and well behaved convergence is observed with increase in the orders of numerator and denominator of Padé approximation. The timings for the calculations performed using CBS3DS and Padé approximations are given in Table 1. Note that the timings for Taylor series expansion and Padé approximation are the same except for the cost of calculating Padé coefficients from the Taylor

15

series coefficients. It is observed that the cost of generating moments and the Pade coefficients is very minute compared to the cost of matrix generation and solution.

(b) Circular Cavity: A circular cavity (*radius=0.305cm and height=0.3cm*) in an infinite ground plane is considered (fig. 4a). The discretization of the circular cavity resulted in 1327 total unknowns, and the order of the dense matrix due to MoM is 132. Backscattering from this cavity is calculated over the frequency range 10GHz to 50GHz with the incident angle $\theta = 0^o$ and $\phi = 0^o$ and plotted in Figure 4b. The Taylor series moments are calculated at 30GHz. Taylor series expansion is calculated with five moments and the Padé approximation is calculated with *L=3* and *M=2*. It can be seen that Padé approximation could give accurate results throughout the frequency range, whereas Taylor series gave accurate results only within the frequency range 21GHz to 39GHz. The timings for calculation of backscattering cross section using "exact method" and the Padé approximation are given in Table 1.

(c) Rectangular cavity with lossy material: A rectangualr cavity is considered as another example (fig. 2 with *a=1cm, b=0.25cm,* and *c=0.25cm*). The cavity is filled with lossy material with dielectric constants $\varepsilon_r = 2.2 - j1.5$ and $\mu_r = 1.8 - j0.1$. The cavity is discretized using tetrahedral elements resulting in 3218 unknowns. The order of the dense matrix due to MoM is 275. The backscatter cross section is calculated over the frequency range 10GHz to 50GHz with the incident angle $\theta = 0^o$ and $\phi = 0^o$ and plotted in Figure 5a. The incident wave is assumed to be H-polarized. Taylor series expansion is calculated with five moments at 30GHz and accordingly the Padé approximation is calculated with *L=3* and *M=2*. It can be seen that Padé approximation gave accurate results throughout the frequency range, whereas Taylor series gave accurate results only within the frequency range 22GHz and 38GHz. The backscattering cross

16

section calculations are also carried out for an E-polarized incident wave with incident angle $\theta = 0^o$ and $\phi = 0^o$ and plotted in Figure 5b. Padé approximation is calculated with *L=5* and *M=4*. Taylor series approximation is calculated with nine moments at 30GHz. It can be seen even for this case that Padé approximation gave accurate results throughout the frequency range 10GHz to 50GHz, whereas Taylor series is accurate only within the frequency range 20GHz to 38GHz. The timings for calculation of backscattering cross section using "exact method" and the Padé approximation are given in Table 1. The discretization for the "exact" calculations using CBS3DS at frequency points beyond 40GHz resulted in 5848 unknowns and order of the dense matrix due to MoM is 421. It can be noted that both Taylor series and Padé approximation are evaluated at 30GHz and hence the dicretization that is used at 30GHz is accurate enough to calculate the hybrid FEM-MoM matrix and the derivative matrices. The results obtained using Padé approximation show a good agreement with the "exact" calculations with denser gridding even beyond 40GHz.

Comment on Storage: In all the above examples, when solving a matrix equation, one needs to store the matrix $A(k_o)$ for exact solution at each frequency. For n^{th} order AWE, one needs to store *n* number of matrices $(A^{(q)}(k_o)$, *q=1,2,3,...n*), along with the matrix $A(k_o)$. For electrically large problems, this could impose a burden on computer resources. This problem can be overcome by storing the derivative matrices, $A^{(q)}(k_o)$ out-of-core, as the derivative matrices are required only for matrix-vector multiplication.

Table 1: Comparison of CPU timings for the numerical examples presented in Sections 4a, b and c

Problem	Method	Matrix Fill (secs)	LU Factor (secs)	Total Time (secs)
(a) Rectangular cavity *(a=1cm, b=0.5cm, c=0.5cm)*	CBS3DS (13 freq. points)	2081.7	312.0	2393.7
	Padé(L=5, M=5) (100 freq. points)	354.7	25.0	379.7
(b) Circular cavity *(radius=0.305cm, height=0.3cm)*	CBS3DS (41 freq. points)	6342.7	270.60	6613.3
	Padé(L=3,M=2) (400 freq. points)	323.7	6.64	330.34
(c) Material filled rectangular Cavity *(a=1cm,b=0.25cm, c=0.25cm)*	CBS3DS (41 freq. points)	19526.9 (10GHz-40GHz) + 14880.0 (41GHz-50GHz)	1110.73 (10GHz-40GHz) + 1413.5 (41GHz-50GHz)	37021.13
	Padé(L=3,M=2) (400 freq. points) **(H-Pol)**	1330.1	34.67	1364.77
	Padé(L=5,M=4) (400 freq. points) **(E-Pol)**	1429.21	34.67	1463.88

5. Concluding Remarks

The AWE technique is applied to the hybrid FEM/MoM technique to calculate the radar cross section of a cavity-backed aperture over a frequency range. Examples of a rectangular cavity, a circular cavity, and a material filled cavity are considered to validate the analysis. Both Taylor series approximation and Padé approximation are calculated for all the examples. It can be noted that for the same computational effort, the Padé approximation proved to be superior in terms of wider bandwidth. Timing comparisons are done for calculating radar cross section over a frequency range using AWE and using 'exact' calculation at each frequency point. AWE is found to be superior in terms of the CPU time. It may be noted that although calculations are done in frequency increments of 0.1GHz for eamples presented in this paper, frequency response at even finer increments can also be calculated at a very nominal cost. This is particularly important when there are sharp nulls present in the frequency response.

Appendix

Derivatives of *A(k)* and *b(k)* w.r.t. *k*

The frequency derivatives of *A(k)* and *b(k)* are evaluated and are given below. From equation (4):

$$A^{(q)}(k) = \frac{d^q A(k)}{dk^q} = A_1^{(q)}(k) + A_2^{(q)}(k) + A_3^{(q)}(k) + A_4^{(q)}(k) \quad q=0,1,2,3,........ \quad \text{(A.1)}$$

From equation (5)

$$A_1^{(0)}(k) = \iiint\limits_V \frac{1}{\mu_r}(\nabla\times\mathbf{T}) \bullet (\nabla\times\mathbf{E})\,dv - k^2\varepsilon_r\iiint\limits_V \mathbf{T}\bullet\mathbf{E}\,dv \quad\quad \text{(A.2)}$$

$$A_1^{(1)}(k) = -2k\varepsilon_r\iiint\limits_V \mathbf{T}\bullet\mathbf{E}\,dv \quad\quad \text{(A.3)}$$

$$A_1^{(2)}(k) = -2\varepsilon_r\iiint\limits_V \mathbf{T}\bullet\mathbf{E}\,dv \quad\quad \text{(A.4)}$$

$$A_1^{(q)}(k) = 0 \quad\quad\quad q \geq 3 \quad\quad \text{(A.5)}$$

From equation (6)

$$A_2^{(0)}(k) = -\frac{k^2}{2\pi}\iint\limits_{S_{ap}} \mathbf{T}_s \bullet \left(\iint\limits_{S_{ap}} \mathbf{M}\frac{\exp(-jkR)}{R}ds' \right)ds \quad\quad \text{(A.6)}$$

$$A_2^{(1)}(k) = \iint\limits_{S_{ap}} \mathbf{T}_s \bullet \left(\iint\limits_{S_{ap}} \mathbf{M}\left(\frac{j}{2\pi}\right)\left[2k + k^2(-jR)\right]\frac{\exp(-jkR)}{(-jR)}ds' \right)ds \quad\quad \text{(A.7)}$$

$$A_2^{(q)}(k) = \iint\limits_{S_{ap}} \mathbf{T}_s \bullet \left(\iint\limits_{S_{ap}} \mathbf{M}\left(\frac{j}{2\pi}\right)\left[\frac{q!}{(q-2)!}(-jR)^{q-3} + 2qk(-jR)^{q-2} + k^2(-jR)^{q-1}\right]\exp(-jkR)\,ds' \right)ds \; \text{for } q>1 \text{ (A.8)}$$

From equation (7)

$$A_3^{(0)}(k) = \frac{1}{2\pi} \int\!\!\int_{S_{ap}} (\nabla \cdot \mathbf{T}_s) \left\{ \int\!\!\int_{S_{ap}} (\nabla' \cdot \mathbf{M}) \frac{\exp(-jkR)}{R} ds' \right\} ds \tag{A.9}$$

$$A_3^{(q)}(k) = \int\!\!\int_{S_{ap}} (\nabla \cdot \mathbf{T}_s) \left\{ \int\!\!\int_{S_{ap}} (\nabla' \cdot \mathbf{M}) \left(-\frac{j}{2\pi} \right) (-jR)^{(q-1)} \exp(-jkR)\, ds' \right\} ds \tag{A.10}$$

From equation (8)

$$b^{(0)}(k) = 2j\omega\mu_o \int\!\!\int_{S_{ap}} (\mathbf{T} \times \hat{\mathbf{n}}) \cdot \mathbf{H}_{inc}\, ds \tag{A.11}$$

Noting from equation (9) that

$$\mathbf{H}_{inc} = \mathbf{H}_i e^{jk(x_1 + y_1 + z_1)} \tag{A.12}$$

where

$$\mathbf{H}_i = \hat{\mathbf{x}} H_{xi} + \hat{\mathbf{y}} H_{yi} + \hat{\mathbf{z}} H_{zi}$$

$$x_1 = x \sin\theta_i \cos\phi_i$$

$$y_1 = y \sin\theta_i \sin\phi_i$$

and

$$z_1 = z \cos\theta_i$$

Equation (A.11) can be rewritten as

$$b^{(0)}(k) = 2jk\eta_o \int\!\!\int_{S_{ap}} (\mathbf{T} \times \hat{\mathbf{n}}) \cdot \mathbf{H}_i e^{jk(x_1 + y_1 + z_1)}\, ds \tag{A.13}$$

For $q \neq 0$

$$b^{(q)}(k) = \frac{d^q b(k)}{dk^q} = 2q\,(j)^q \eta_o \iint\limits_{S_{ap}} (\mathbf{T} \times \hat{\mathbf{n}}) \cdot \mathbf{H}_i \, (x_1 + y_1 + z_1)^{(q-1)} \, e^{jk\,(x_1 + y_1 + z_1)} \, ds$$

$$+ 2k\eta_o\,(j)^{q+1} \iint\limits_{S_{ap}} (\mathbf{T} \times \hat{\mathbf{n}}) \cdot \mathbf{H}_i \, (x_1 + y_1 + z_1)^{q} \, e^{jk\,(x_1 + y_1 + z_1)} \, ds \qquad \text{(A.14)}$$

References

[1]   T.B.A.Senior, "Electromagnetic field penetration into a cylindrical cavity," *IEEE Trans. Electromagnetic Compat.*, Vol.EMC-18, pp.71-73, May 1976.

[2]   J.R.Mautz and R.F.Harrington, "Electromagnetic penetration into a conducting circular cylinder through a narrow slot, TM case," *J. Electromagn. Wave Appl.*, Vol.2, no.3/4,pp.269-293, 1988.

[3]   J.M.Jin and J.L.Volakis, "TE scattering by an inhomogeneously filled aperture in a thick conducting ground plane," I*EEE Trans. Antennas and Propagation*, vol.38, pp.280-286, Aug. 1990.

[4]   J.M.Jin and J.L.Volakis, "TM scattering by an inhomogeneously filled aperture in a thick conducting ground plane," *Proc. Inst. Elec. Eng.,* pt.H, vol.137, pp.153-159, June 1990.

[5]   S.K.Jeng, "Scattering from a cavity backed slit in a ground plane-TE case," *IEEE Trans. Antennas and Propagation.*, vol.38, pp.1523-1529, Oct. 1990.

[6]   T.M.Wang and H.Ling, "A connection algorithm on the problem of EM scattering from arbitrary cavities," *J. Electromagnetic Wave Appl.*, vol.5, no.3, pp.301-314, 1991.

[7]   S.W.Lee and H.Ling, *Data book for cavity RCS (version 1),* Univ. Illinois, Electromagn. Lab., Tech. Rep. SWL89-1, Jan 1, 1989.

[8]   R.W.Ziolkowski and W.A.Johnson, "Electromagnetic scattering of an arbitrary plane wave from a spherical shell with a circular aperture," *J. Math Phys.,* Vol. 28, No.6, pp.1263-1314, 1988.

[9]   K.Barkeshli and J.L.Volakis, "Electromagnetic scattering from an aperture formed by a rectangular cavity recessed in a ground plane," *Journal Electromag. Waves Appl.*, Vol.5, No.7, pp.715-734, 1991.

[10] T.M.Wang and H.Ling, "Electromagnetic scattering from three dimensional cavities via a connection scheme," *IEEE Trans. Antennas and Propagation*, vol.39, pp.1505-1513, October 1991.

[11] H.Ling, R.C.Chou and S.W.Lee, "Shooting and bouncing rays: calculating RCS of an arbitrarily shaped cavity," *IEEE Trans. Antennas and Propagation*, vol.37, pp.194-205, Feb 1989.

[12] P.H.Pathak and R.J.Burkholder, "Modal, ray and beam techniques for analyzing the EM scattering by open ended waveguide cavities," *IEEE Trans. Antennas and Propagation,* vol.37, pp.635-647, May 1989.

[13] A.Teflove and K.R.Umashankar, "The finite difference time domain(FD-TD) method for electromagnetic scattering and interaction problem," *J. Electromagn. Waves Appl.*, vol.1, no.4, pp.363-387, 1987.

[14] J.M.Jin and J.L.Volakis, "A finite element-boundary integral formulation for scattering by three dimensional cavity backed apertures," *IEEE Trans. Antennas and Propagation,* vol.39, pp.97-104, Jan. 1991.

[15] E. Chiprout and M. S. Nakhla, *Asymptotic Waveform Evaluation*, Kulwar Academic Publishers, 1994.

[16] G.J.Burke, E.K.Miller, S.Chakrabarthi and K.Demarest, "Using model-based parameter estimation to increase the efficiency of computing electromagnetic transfer functions," *IEEE Trans. Magnetics*, Vol.25, pp.2807-2809, July 1989.

[17] J. Gong and J.L. Volakis, "AWE implementation for electromagnetic FEM analysis," *Electronics Letters*, Vol.32, pp.2216-2217, Nov. 1996.

[18] S.V.Polstyanko, R.Dyczij-Edlinger and J.F.Lee, "Fast frequency sweep technique for the efficient analysis of dielectric waveguides," *IEEE Trans. on Microwave Theory and Technique*s, Vol.45, pp.1118-1126, July 1997.

[19] C.R.Cockrell and F.B.Beck, "Asymptotic Waveform Evaluation (AWE) technique for frequency domain electromagnetic analysis," *NASA Technical Memorandum 110292,* November 1996.

[20] C. J. Reddy and M. D. Deshpande, "Application of AWE for RCS frequency response calculations using Method of Moments," *NASA Contractor Report 4758*, October 1996.

[21] C. J. Reddy and M. D. Deshpande, "Frequency response calculations of input characteristics of cavity-backed aperture antennas using AWE with hybrid FEM/MoM technique," *NASA Contractor Report 4764,* January 1997.

[22] J.M.Jin, *Finite Element Method in Electromagnetics,* John Wiley & Sons, 1993.

[23] R.F.Harrington, *Time Harmonic Electromagnetic Fields*, McGraw Hill Inc, 1961.

[24] S.M.Rao, D.R.Wilton and A.W.Glisson, "Electromagnetic scattering by surfaces of arbitrary shape," *IEEE Trans. Antennas and Propagation*, Vol.AP-30, pp.409-418, May 1982.

[25] C.J.Reddy and M.D.Deshpande, "User's Manual for CBS3DS-Version 1.0," *NASA Contractor Report 198236*, October 1995.

[26] O. O. Storaasli, "Performance of NASA equation solvers on computational mechanics applications ," *American Institute of Aeronautics and Astronautics (AIAA) Paper No. 96-1505*, April, 1996.
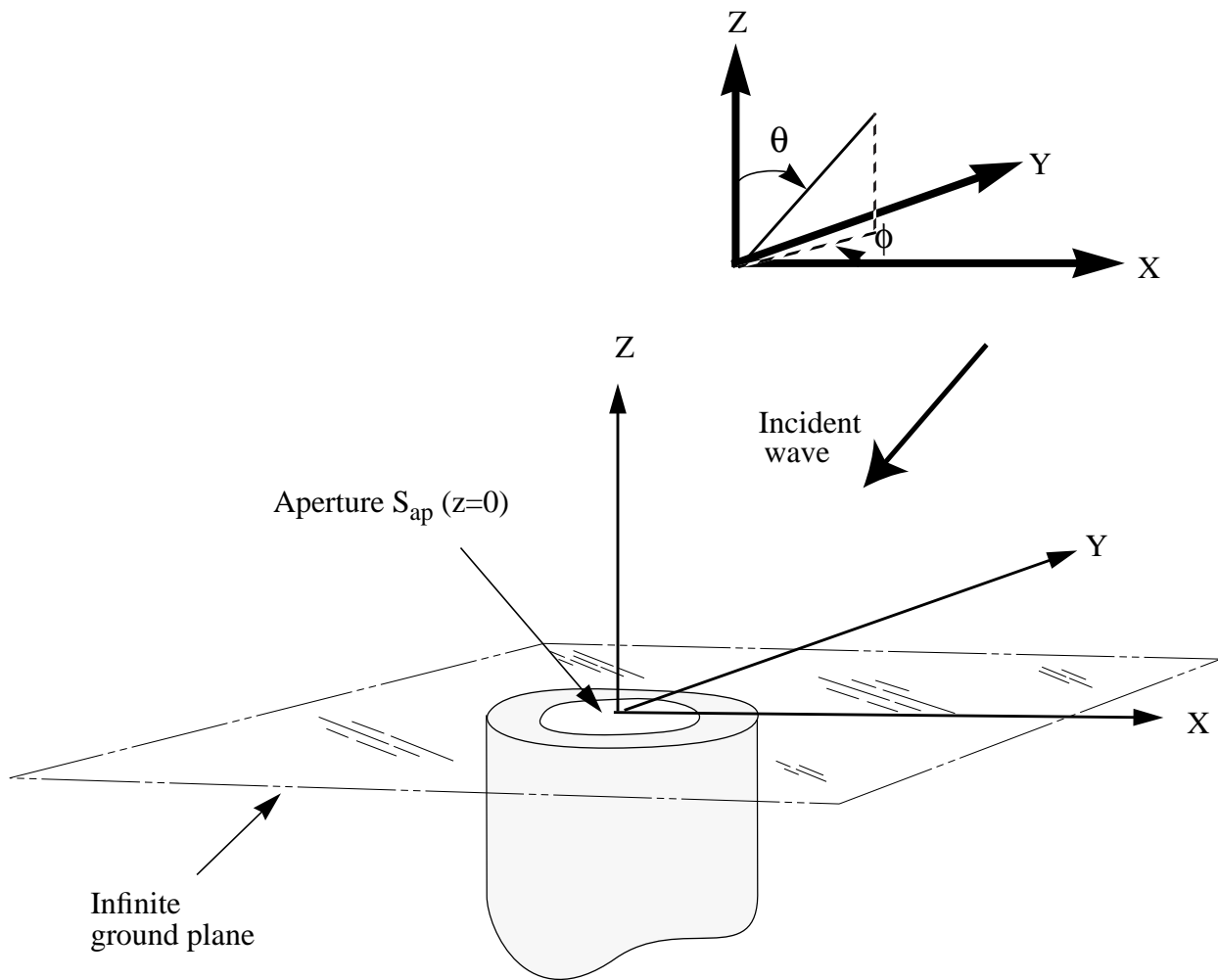
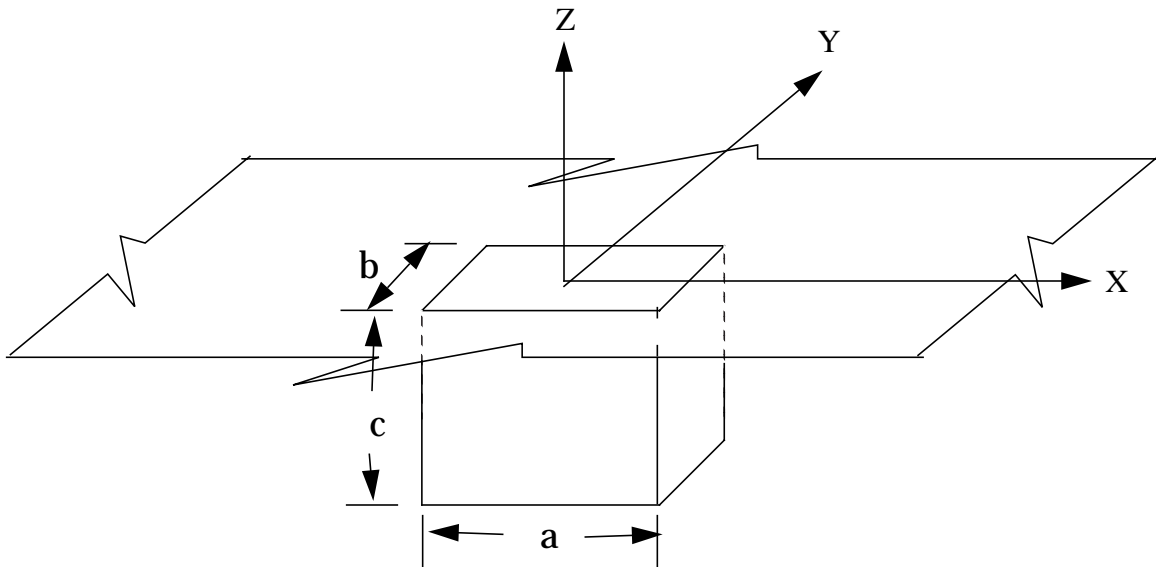Figure 1 Geometry of a cavity-backed arbitrarily shaped aperture in an infinite ground plane.

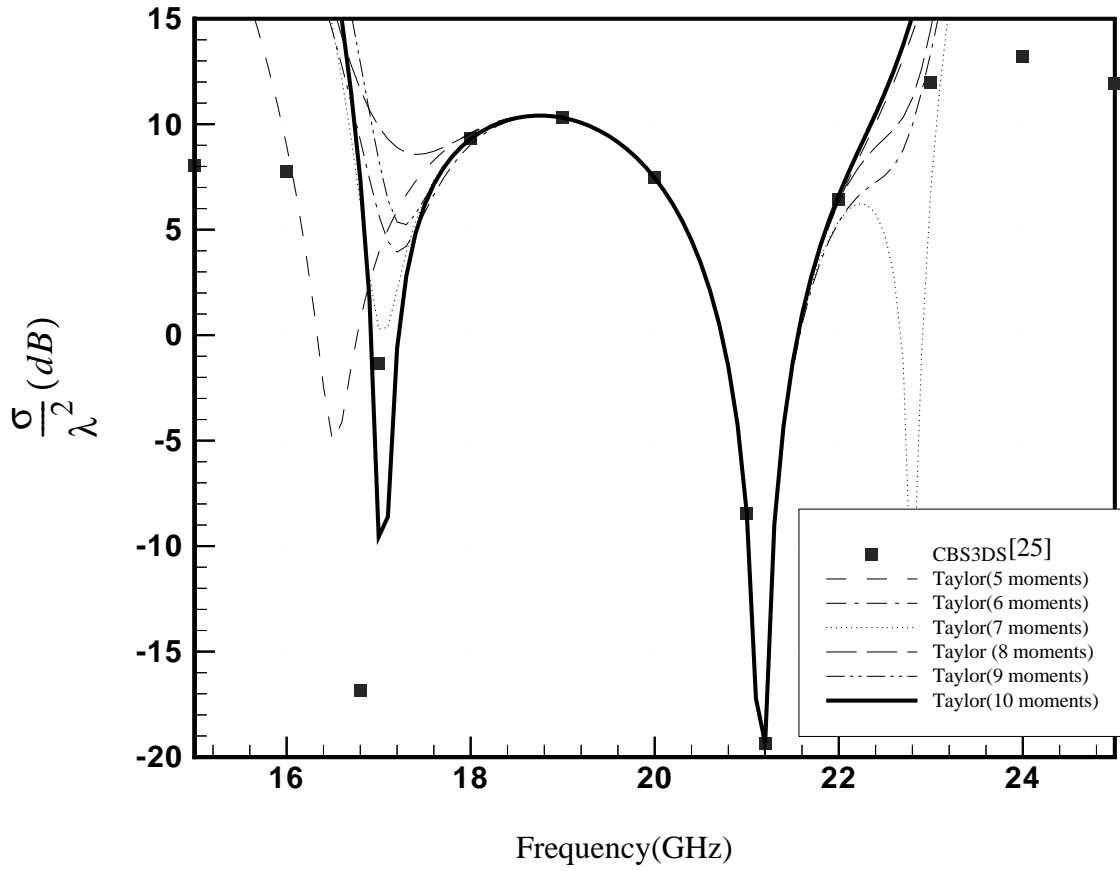Fig. 2 Geometry of the rectangular cavity backed aperture.

Figure 3a   Frequency response calculation for the rectangular cavity shown in figure 2 (*a=1cm, b=1cm, c=2cm*, ε_r*=1.0*, μ_r*=1.0*) using Taylor series approximation.
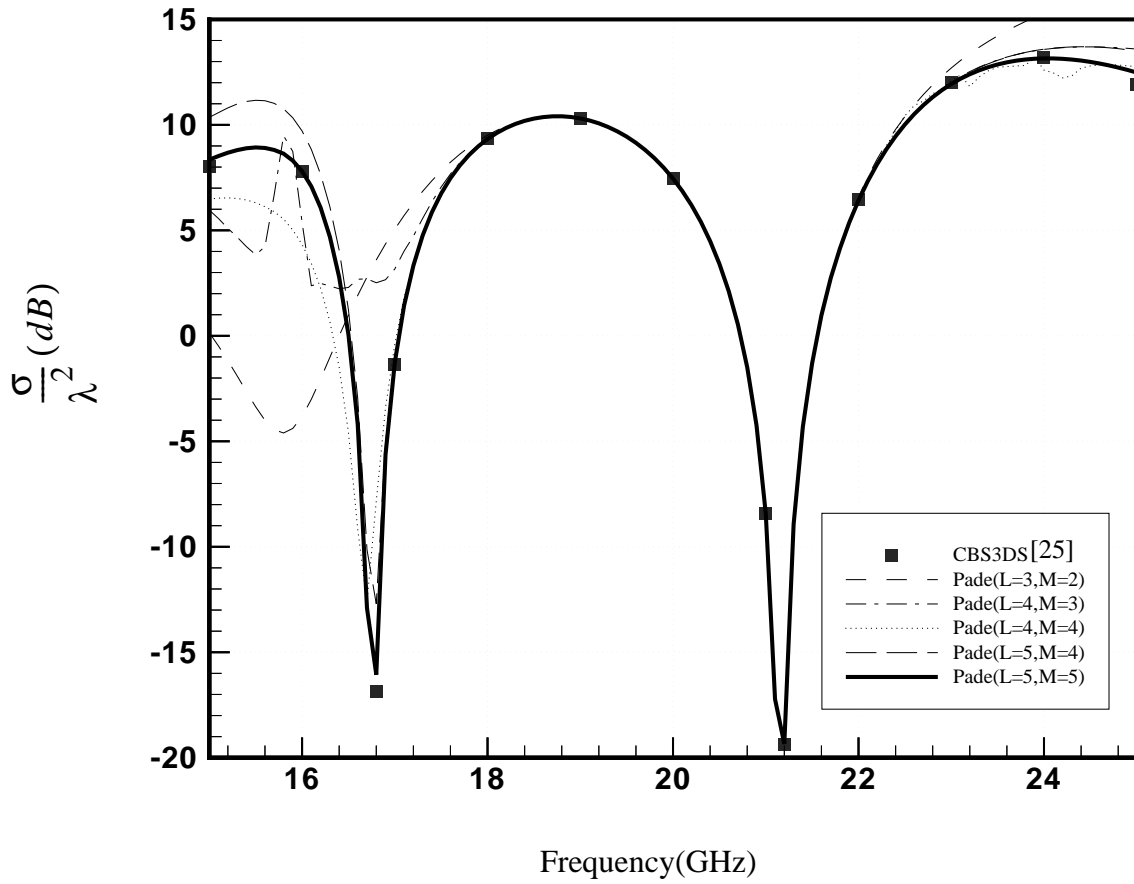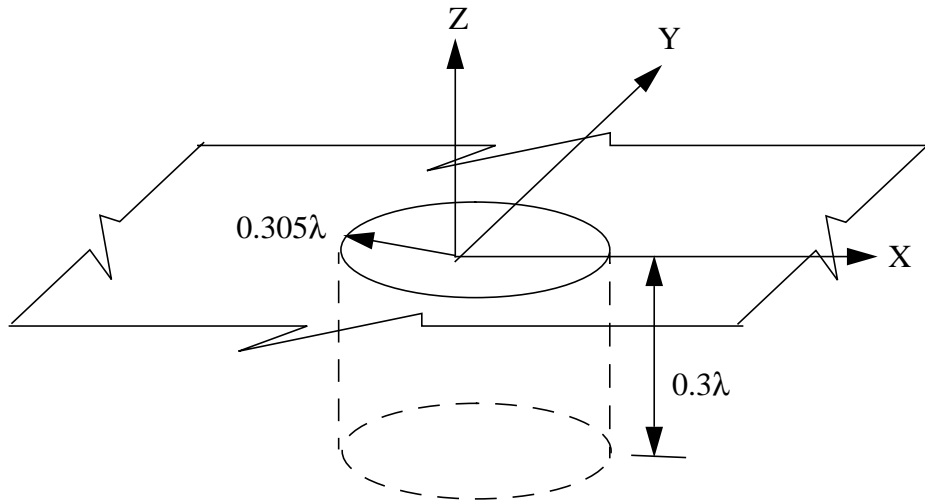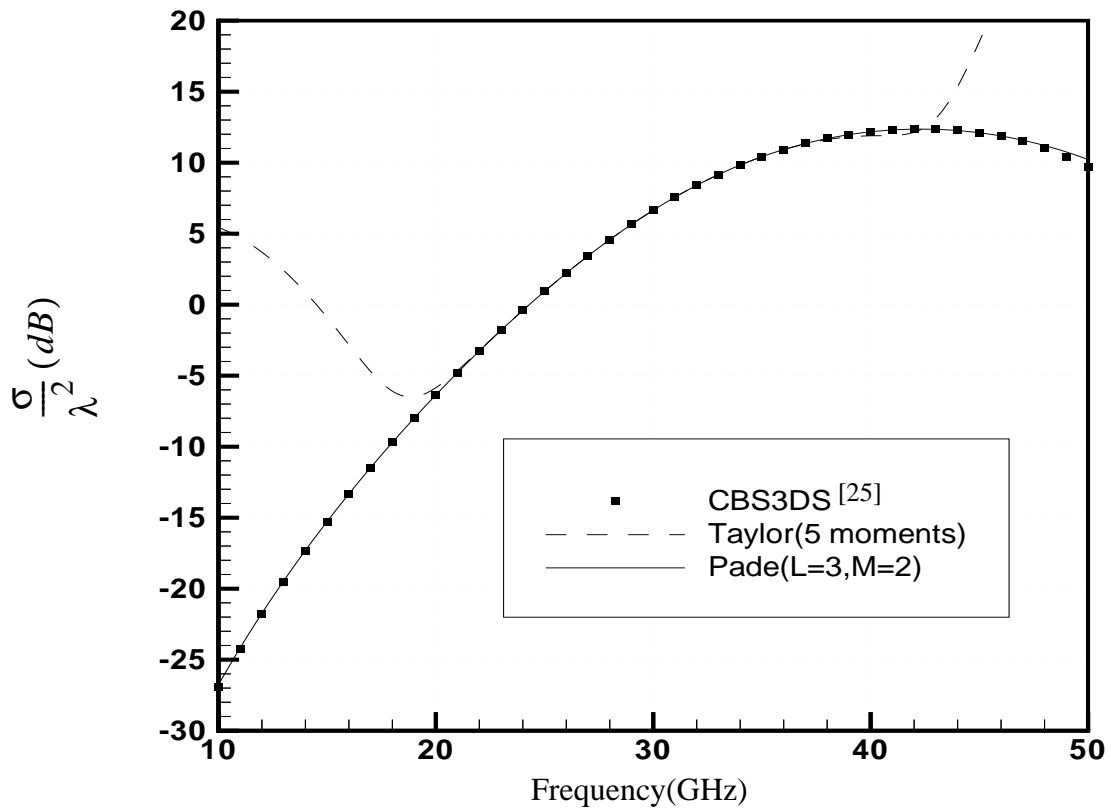
Figure 3b Frequency response calculation for the rectangular cavity shown in figure 2 (*a=1cm, b=1cm, c=2cm, ε_r=1.0, μ_r=1.0*) using Padé approximation.

(a)

(b)

Figure 4. Frequency response calculations of back scattering from an air-filled circular cavity. (a) Geometry of the circular cavity (b) Backscattering cross section versus frequency.
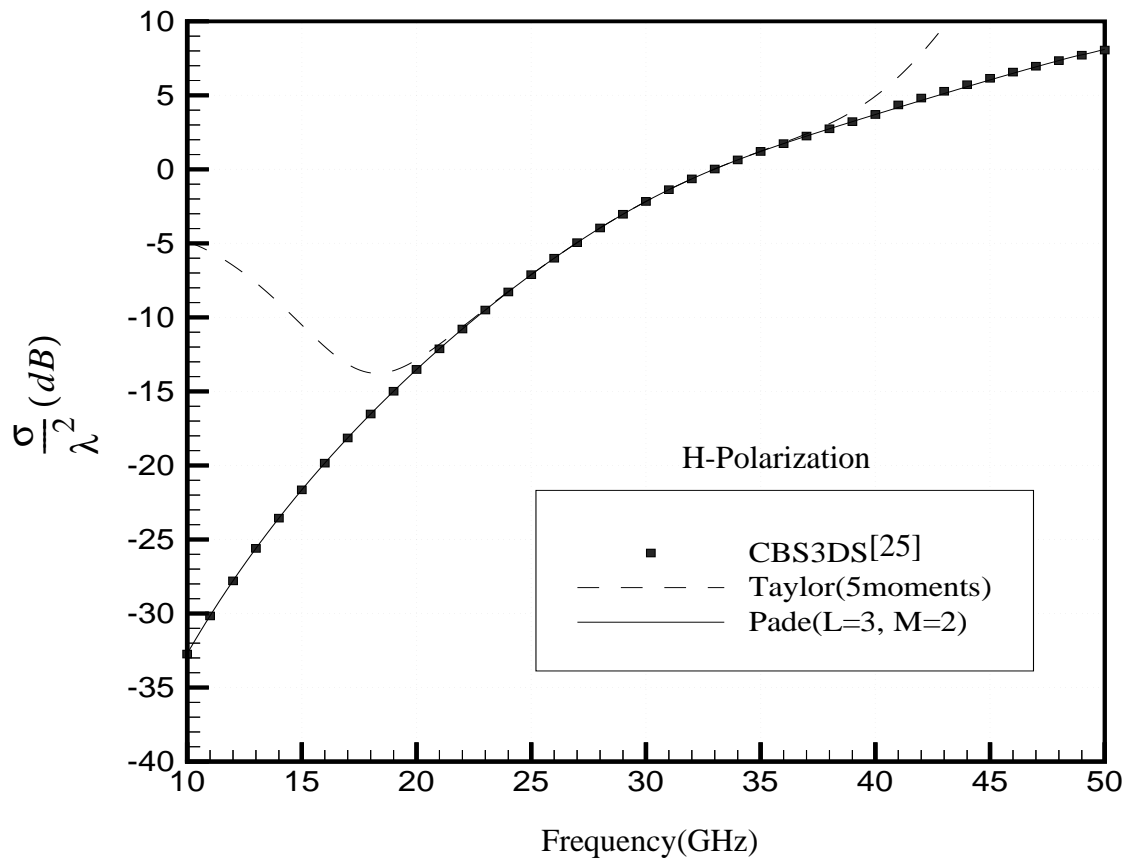
Figure 5a Frequency response calculation for the rectangular cavity shown in figure 2 (*a=1cm,*
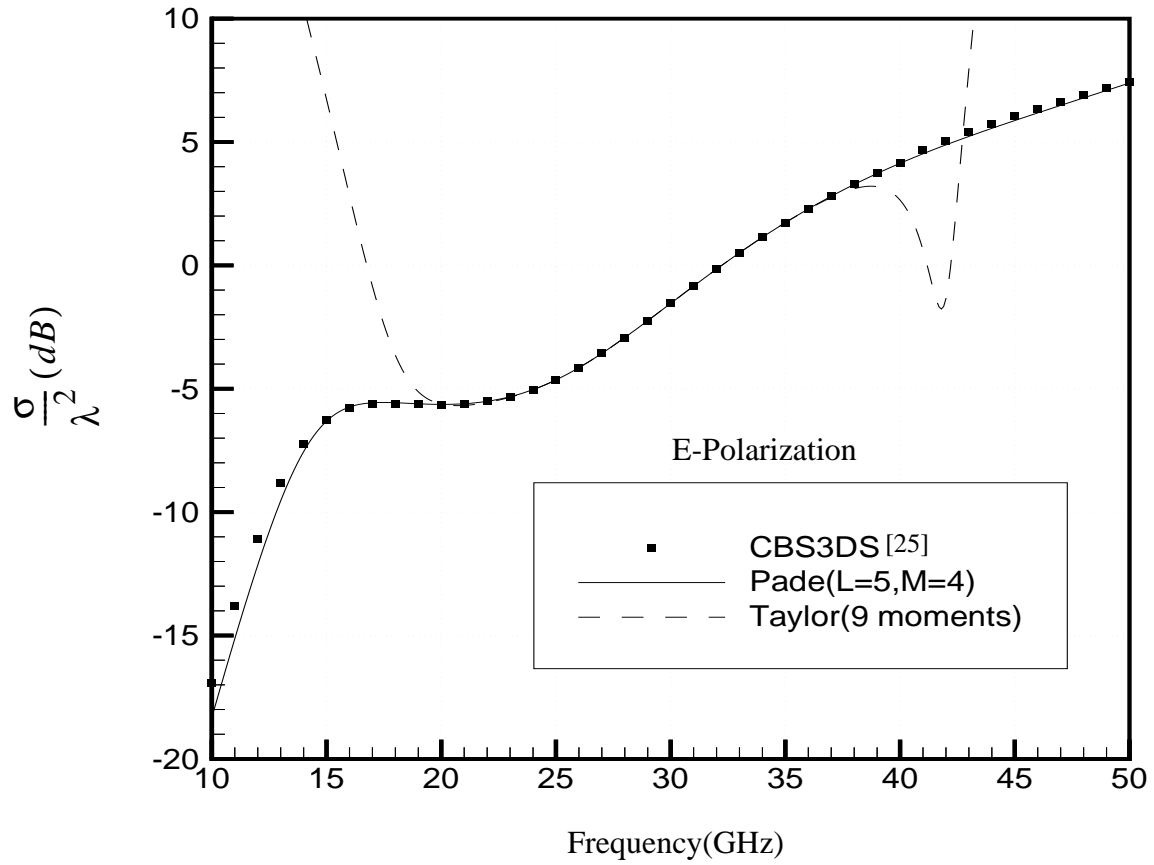*b=0.25cm, c=0.25cm,* ε_r*=2.2-j1.5,* μ_r*=1.8-j0.1*). H-Polarization

Figure 5b Frequency response calculation for the rectangular cavity shown in figure 2 (*a=1cm, b=0.25cm, c=0.25cm, ε_r=2.2-j1.5, μ_r=1.8-j0.1*). E-Polarization.

REPORT DOCUMENTATION PAGE

Public reporting burden for this collection of information is estimated to average 1 hour per response, including the time for reviewing instructions, searching existing data sources, gathering and maintaining the data needed, and completing and reviewing the collection of information. Send comments regarding this burden estimate or any other aspect of this collection of information, including suggestions for reducing this burden, to Washington Headquarters Services, Directorate for Information Operations and Reports, 1215 Jefferson Davis Highway, Suite 1204, Arlington, VA 22202-4302, and to the Office of Management and Budget, Paperwork Reduction Project (0704-0188), Washington, DC 20503.

1. AGENCY USE ONLY (Leave blank)	2. REPORT DATE	3. REPORT TYPE AND DATES COVERED
	December 1997	Contractor Report

4. TITLE AND SUBTITLE

Application of AWE Along with a Combined FEM/MoM Technique to Compute RCS of a Cavity-Backed Aperture in an Infinite Ground Plane Over a Frequency Range

5. FUNDING NUMBERS

NCC1-231

522-11-41-02

6. AUTHOR(S)

C. J. Reddy and M. D. Deshpande

7. PERFORMING ORGANIZATION NAME(S) AND ADDRESS(ES)

Hampton University
Hampton, Virginia

8. PERFORMING ORGANIZATION REPORT NUMBER

9. SPONSORING/MONITORING AGENCY NAME(S) AND ADDRESS(ES)

National Aeronautics and Space Administration
NASA Langley Research Center
Hampton, VA 23681-2199

10. SPONSORING/MONITORING AGENCY REPORT NUMBER

NASA/CR-97-206261

11. SUPPLEMENTARY NOTES

Langley Technical Monitor: Fred B. Beck

12a. DISTRIBUTION/AVAILABILITY STATEMENT

Unclassified-Unlimited
Subject Category 32   Distribution: Non-Standard
Availability: NASA CASI (301) 621-0390

12b. DISTRIBUTION CODE

13. ABSTRACT (Maximum 200 words)

A hybrid Finite Element Method (FEM)/Method of Moments (MoM) technique in conjunction with the Asymptotic Waveform Evaluation (AWE) technique is applied to obtain radar cross section (RCS) of a cavity-backed aperture in an infinite ground plane over a frequency range. The hybrid FEM/MoM technique when applied to the cavity-backed aperture results in an integro-differential equation with electric field as the unknown variable, the electric field obtained from the solution of the integro-differential equation is expanded in Taylor series. The coefficients of the Taylor series are obtained using the frequency derivatives of the integro-differential equation formed by the hybrid FEM/MoM technique. The series is then matched via the Padé approximation to a rational polynomial, which can be used to extrapolate the electric field over a frequency range. The RCS of the cavity-backed aperture is calculated using the electric field at different frequencies. Numerical results for a rectangular cavity, a circular cavity, and a material filled cavity are presented over a frequency range. Good agreement between AWE and the exact solution over the frequency range is obtained.

14. SUBJECT TERMS

Asymptotic Waveform Evaluation, Padé Approximation, Finite Element Method, Method of Moments, Hybrid Method, Cavity-Backed Apertures, Radar Cross Section

15. NUMBER OF PAGES

37

16. PRICE CODE

A03

17. SECURITY CLASSIFICATION OF REPORT	18. SECURITY CLASSIFICATION OF THIS PAGE	19. SECURITY CLASSIFICATION OF ABSTRACT	20. LIMITATION OF ABSTRACT
Unclassified	Unclassified	Unclassified	